The Anomeric Effect in Seven-Membered Rings: A Conformational Study of 2-Oxa Derivatives of Benzocycloheptene by NMR

S. Désilets and M. St-Jacques*

Contribution from the Département de Chimie, Université de Montréal C.P. 6128, Succ. "A", Montréal, Québec, Canada H3C 3J7. *Received July 21, 1986*

Abstract: The conformational consequences of the anomeric effect are determined for 3-methoxy-1,3,4,5-tetrahydro-2-benzoxepin (**7**) by using ^1H and ^{13}C dynamic NMR techniques, two-dimensional COSY spectra at low temperatures, and computer simulation of spectral modifications. Whereas the parent compound **6** exists solely in the chair conformation, methoxy substitution leads to three conformations for **7** (C_a, C_e, and TB). It is shown that both the C_a and TB forms are stabilized by stereoelectronic factors. The results for 7 are compared with those for 2-methoxytetrahydropyran (**8**), and this illustrates the consequences of the anomeric effect not manifested in six-membered rings. Solvent-induced conformational changes are explained in terms of attenuation of the electrostatic component to the anomeric effect suggesting little perturbation of the orbital component. The stabilization by the single methoxy substituent of the TB conformation not present in the parent compound **6** warns of the potential complexity that could exist in larger flexible rings.

Previous results[1,2] for the 2,4-benzodioxepins **1**–**4** have shown strikingly different conformational features depending on the nature of the substituents. Whereas **1** and **3** exist predominantly in the chair (C) conformation in CHF_2Cl solutions, both **2** and **4** were found to exist solely in the twist-boat (TB) form. It was deemed that steric repulsion governs the TB conformational preference of **2** while the conformational properties of **4** were believed to be of stereoelectronic origin. Furthermore, it has been found that changing the location of the two ring oxygens as in **5** leads to yet another behavior.[3] Indeed **5** has been reported to exist as a mixture of C_e and C_a forms in the ratio of 88:12 in CH_3OCH_3 at −132 °C while only the C_e form has been detected in CHF_2Cl.

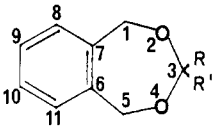

1 R = R' = H

2 R = R' = CH_3

3 R = H ; R' = CH_3

4 R = H ; R' = OCH_3

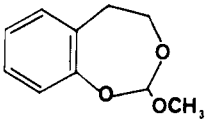

5

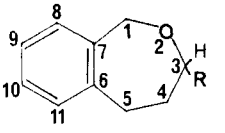

6 R = H

7 R = OCH_3

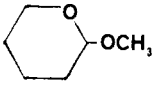

8

In order to better assess the importance of the anomeric effect in seven-membered rings, the 2-benzoxepins **6** and **7** were prepared and investigated by variable temperature high field ^1H and ^{13}C NMR methods. The fact that the ring structure of **6** and **7** contains only one ring oxygen atom suggests that the results for **7** should provide specific information amenable to a comparison with those for **8**, whose conformational properties have been amply studied[4] and which presently serves as a model describing the basic tenets of the anomeric effect.[5] Our observations for **7** show marked differences with those reported for **8**, so that they provide new insight into the importance of the underlying stereoelectronic phenomenon in flexible ring systems.

Results and Spectral Analyses

Both compounds **6** and **7** gave dynamic NMR spectral changes at low temperatures. In the case of **6**, only the ^1H spectrum is modified, whereas for **7**, both the ^1H and ^{13}C spectra revealed changes. Spectral parameters for these compounds are listed in Tables I and II.

Spectra of 6. The proton decoupled room temperature ^{13}C NMR spectrum of **6** at 100.62 MHz was analyzed by using data from the coupled spectrum, off-resonance decoupling, and selective heteronuclear double irradiation techniques.[6] Analysis of reduced couplings (^1J_r) lead to the assignment of the aliphatic portion of the spectrum while perturbation associated with long range couplings lead to the assignment of the aromatic carbons. The assigned chemical shifts are summarized in Table I. No spectral modification was detected at −125 °C, suggesting the existence of a single conformation for **6**.

Figure 1 illustrates the 400.13-MHz ^1H NMR spectral modification observed for the aliphatic protons of **6** in CHF_2Cl. Assignment of the signals at −20 °C is straightforward, and the result is shown in the figure. The spectrum at −125 °C shows that the H-1 singlet has changed into an AB quartet whereas the other aliphatic proton signals have split into two multiplets of equal intensity.

The low-temperature spectrum indicates that the protons of each methylene groups are nonequivalent in the molecular conformation adopted by **6**. Spectral analysis leads to the assignments shown in the figure and yields the parameters given in Table II. These parameters and additional arguments in the discussion section show clearly that the conformation of **6** is the chair **9** and the symbols a and e refer to axial and equatorial protons.

Spectra of 7. The 100.62-MHz ^{13}C NMR spectrum of **7** in CHF_2Cl, shown in Figure 2, reveals two spectral changes whereby all five sp^3 carbon signals (C-1, C-3, C-4, C-5, and CH_3) have

(1) Blanchette, A.; Sauriol-Lord, F.; St-Jacques, M. *J. Am. Chem. Soc.* **1978**, *100*, 4055.
(2) St-Amour, R.; St-Jacques, M. *Can. J. Chem.* **1983**, *61*, 109.
(3) St-Amour, R.; Phan Viet, M. T.; St-Jacques, M. *Can. J. Chem.* **1984**, *62*, 2830.
(4) (a) Booth, H.; Grindley, T. B.; Knedhair, K. A. *J. Chem. Soc., Chem. Commun.* **1982**, 1047. (b) Sauriol-Lord, F.; St-Jacques, M., unpublished results quoted in F. Sauriol's Ph.D. Thesis, Université de Montréal, 1980. (c) Abe, A. *J. Am. Chem. Soc.* **1976**, *98*, 6477.
(5) Kirby, A. J. *The Anomeric Effect and Related Stereoelectronic Effects at Oxygen*; Springer-Verlag: Berlin, Heidelberg, New York, 1983.
(6) Wehrli, F. W.; Wirthlin, T. *Interpretation of Carbon-13 NMR Spectra*; Heyden: 1978; and references cited therein.

0002-7863/87/1509-1641$01.50/0

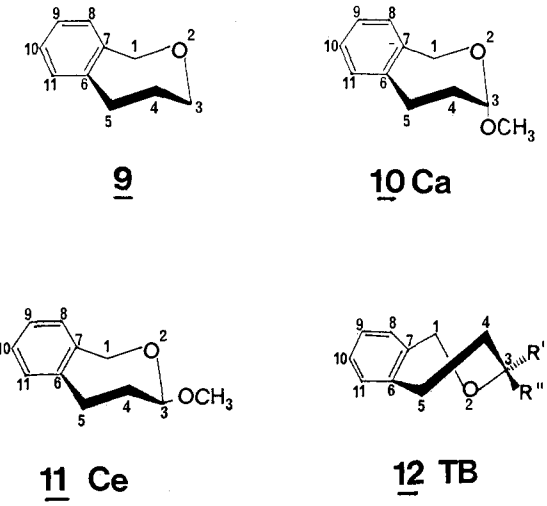

split into three lines of unequal intensity with a 50:27:23 ratio at −120 °C. These lines are labeled C_a, TB, and C_e, respectively, in conformity with their assignment to three conformations made later. A similar spectral change was observed by using CH_3OCH_3 as solvent; the intensities of the C_a, TB, and C_e lines at −120 °C had, however, changed to 61:24:15. Complete analysis of the ^{13}C spectrum will be carried out later, after the ^1H spectral analysis.

Figure 3 illustrates the 400.13-MHz ^1H NMR spectral changes observed for **7** in CHF_2Cl. The spectral assignment of the high-temperature signals shown in the figure and summarized in Table II corresponds to that already published.[7]

The spectral change observed at lower temperatures are complex and give rise to many signals associated with each of the three conformers detected by the ^{13}C NMR spectra. Spectral calculations described in the next section permit a detailed description of the features observed at intermediate temperatures. The assignment of the signals at −120 °C is obtained from the 2D COSY spectral analysis[8] for **7** at −120 °C in CF_2Cl_2 as shown in Figure 4.

Figure 4 shows the contour plot obtained from the 2D COSY experiment together with the normal one-dimensional ^1H spectrum above it. The diagonal peaks correspond to the chemical shifts of the various signals in the normal spectrum while the off-diagonal peaks result from coherence transfer via the *J* coupling.

As starting point for the assignment of the ^1H NMR spectrum of **7**, it is necessary to assign a well-resolved signal. The triplet at 1.67 ppm is selected because its intensity suggests that it belongs to the most abundant conformation, and it can be readily assigned to the axial H-4a proton of the C_a form **10**. Because at −120 °C only large $^2J_{HH}$ and $^3J_{HH}$ couplings are resolved, it follows that the triplet arises from the comparable couplings $^2J_{4a,4e}$ and $^3J_{4a,5a}$. This signal is labeled C_aH-4a in Figure 4; the first part of the label refers to the C_a conformation while the second identifies the proton location and orientation.

A second characteristic signal, also useful as a starting point, is the less intense quartet observed at 1.43 ppm associated with H-4a in the C_e form **11**. In this case, the multiciplicity results from three large coupling constants: $^2J_{4a,4e}$, $^3J_{4a,3a}$, and $^3J_{4a,5a}$.

Starting with the diagonal correlation peak 1, corresponding to the C_a H-4a triplet at 1.67 ppm, the assignment procedure is as follows: The horizontal line joining peaks 1–4 identifies protons coupled to 1 so that signal 2 at 1.9 ppm corresponds to C_aH-4e, signal 3 at 3.4 ppm to C_aH-5a, and signal 4 at 4.7 ppm to C_aH-3.

A correlation also exists between 3 and 5, thus identifying signal 5 at 2.45 ppm to be C_aH-5e. Furthermore, because the C_a form predominates, it is easy to locate the two C_aH-1 signals appearing as doublets at 4.07 and 5.07 ppm and giving rise to the correlation

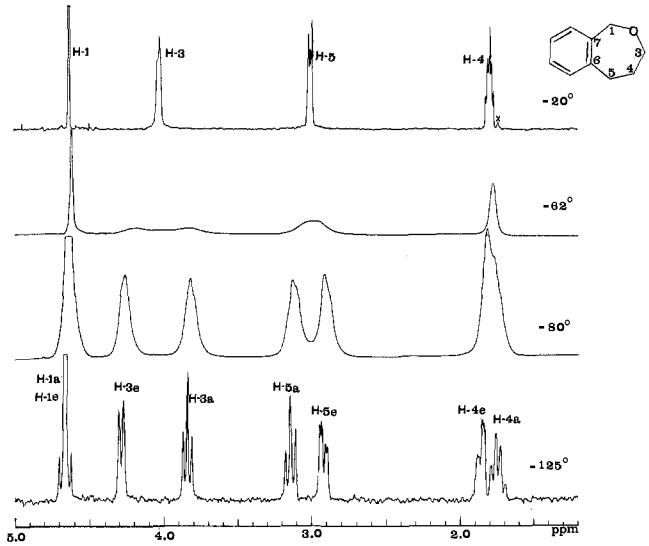

Figure 1. Partial 400.13-MHz ^1H NMR spectra of **6** in CHF_2Cl at several temperatures (× denotes an impurity).

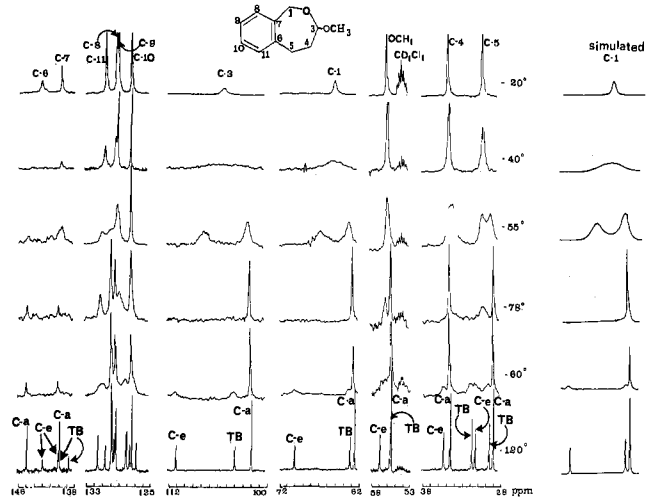

Figure 2. Variable-temperature 100.62-MHz ^{13}C NMR spectra of **7** in CHF_2Cl. (The assignment of the signal between 125 and 133 ppm is given in Table I).

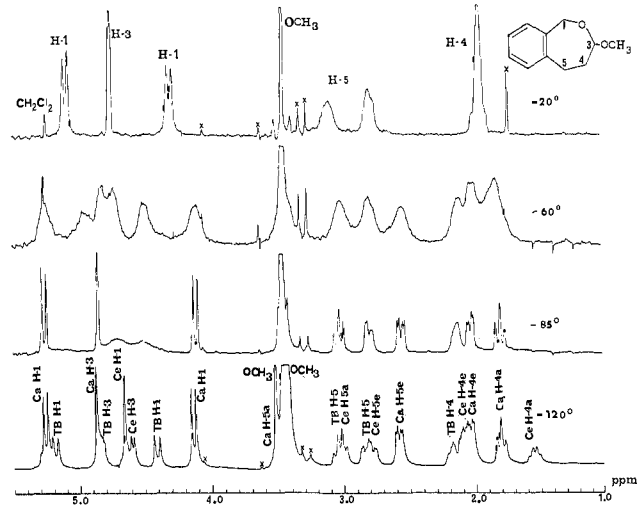

Figure 3. Partial 400.13-MHz ^1H NMR spectra of **7** in CHF_2Cl at several temperatures (× denotes impurities).

peaks 13 and 14. Thus, all seven aliphatic ring protons of the C_a form have been assigned.

The identification of the C_e signals starts with the C_eH-4a quartet at 1.43 ppm giving rise to the diagonal peak 6 in the

(7) Talekar, D. G.; Rao, A. S. *Synthesis* **1983**, 595.
(8) (a) Nagayama, K.; Kumar, A.; Wüthrich, K.; Ernst, R. R. *J. Magn. Reson.* **1980**, *40*, 321. (b) Bax, A.; Freeman, R. *J. Magn. Reson.* **1981**, *44*, 542. (c) Aue, W. D.; Bartholdi, E.; Ernst, R. R. *J. Chem. Phys.* **1976**, *64*, 2229.

Table I. ^{13}C Chemical Shifts[a] for Compounds **6** and **7** at High and Low Temperatures Together with Substituent Parameters

compd	solvent	T (°C)	confmtn[b]	C-1	C-3	C-4	C-5	C-6	C-7	C-8	C-9	C-10	C-11	OCH_3	α	β	γ_{c-1}	γ_{c-5}
6	CH_3OCH_3	−10		75.56	76.24	31.52	36.35	143.74	141.65	129.11	128.36	126.68	129.69					
			C >98%															
(H, H)		−120		75.14	76.19	31.13	35.93	143.86	141.46	129.30	128.55	126.54	129.71					
	CHF_2Cl	−20		76.33	77.13	31.90	36.87	144.73	141.96	129.86	129.32	127.50	130.58					
			C >98%															
		−120		75.70	76.84	31.02	36.15	144.59	141.17	129.73	129.15	127.22	130.32					
7	CH_3OCH_3	−10		64.18	104.12	34.42	29.87	141.84	140.75	128.62	128.21	126.68	129.85	55.05				
(H, OCH_3)		−120	Ca 61%	62.00	101.30	34.43	28.73	144.15	140.80	129.11	128.60	126.75	129.33	54.76	25.1	3.3	−13.1	−7.2
			Ce 15%	69.15	110.25	35.23	30.94	142.26	140.80	129.09	128.75	127.02	129.86	55.90	34.1	4.1	−6.0	−5.0
			TB 24%	62.55	103.44	31.75	29.38	140.15	139.47	127.40[c]	127.34[c]	126.27	130.81	54.86				
	CHF_2Cl	−20		64.95	105.06	34.53	30.11	143.18	140.73	129.05	128.80	127.17	130.37	55.67				
		−120	Ca 50%	62.60	101.94	34.48	28.99	144.88	140.89	129.85	129.36	127.40	129.91	55.49	25.1	3.5	−13.1	−7.2
			Ce 23%	70.04	111.04	35.30	31.35	142.89	141.00	129.63	129.46	127.64	130.68	56.93	34.2	4.3	−5.7	−4.8
			TB 27%	63.15	103.98	31.79	29.55	140.89	139.64	128.10[c]	128.01[c]	126.81	131.55	55.59				
8	CHF_2Cl	−120	Ca[d]												29.6	3.5	−9.0	−5.3
			Ce												35.3	5.3	−2.0	−0.9

[a] Solutions containing internal Me_4Si and CD_2Cl_2 (15–20%) for lock purpose. [b] The symbols C, Ce, Ca, and TB refer to conformations described in the text. [c] The assignment of these signals is uncertain and could be reversed. [d] Data taken from ref 4b.

Table II. ^1H NMR Spectral Parameters for Compounds **6** and **7** in CHF_2Cl

compd	T (°C)	confrmtn	H-1	H-3	H-4	H-5	aromatics	CH_3O
6	−20		4.63 (s)	4.03 (t), $^3J_{3-4}$ = 4.0 Hz	1.79 (m)	3.00 (t), $^3J_{5-4}$ = 5.6 Hz	7.09–7.05 (m)	
(H, H)	−125	C	4.69 and 4.63 (AB pattern), ^2J = −13.5 Hz	3.84 (t, H-3a) ^2J = −11.8 Hz,[a] $^3J_{3a-4a}$ = 12.5 Hz	1.75 (q, H-4a) ^2J = −13 Hz, $^3J_{4a-5a}$ = 13 Hz, $^3J_{4a-3a}$ = 12.5 Hz	3.14 (t, H-5a), ^2J = −14 Hz, $^3J_{4a-5a}$ = 13 Hz	7.09–7.05 (m)	
				4.28 (d, H-3e), $^3J_{3e-4e}$ < 2 Hz	1.86 (dd, H-4e) ^2J = −13 Hz, $^3J_{4e-5e}$ = 5.4 Hz, $^3J_{4e-3e}$ < 2 Hz	2.92 (dd, H-5e) ^2J = −14 Hz, $^3J_{5c-4c}$ = 5.4 Hz		
7	0		5.08 and 4.15 (AB pattern), ^3J = −14.0 Hz	4.67 (t), $^3J_{3-4}$ = 4.0 Hz	1.9 (m)	3.1 and 2.7 (m)	7.2–7.1 (m)	3.45 (s)
(H, OCH_3)	−120	Ca	5.28 and 4.11 (AB pattern), ^2J = −13.5 Hz	4.86 (s, H-3e), $^3J_{3e-4e}$ = nonresolvd	1.80 (t,H-4a), ^2J = −13.4 Hz, $^3J_{4a-5a}$ = 13.4 Hz, 2.1–2.0 (H-4e)[c]	3.4–3.5 (H-5a)[b]	7.2–7.1 (m)	3.45 (s)
						2.58 (dd, H5e), ^2J = −14.0 Hz, $^3J_{5e-4e}$ = 5.5 Hz		
		Ce	4.65 (s, H-1a, H-1e)	4.59 (d, H-3a), $^3J_{3a-4a}$ = 12.0 Hz	1.55 (q, H-4a), ^2J = −12.0 Hz, $^3J_{4a-3a}$ = 12.0 Hz, $^3J_{4a-5a}$ = 12.0 Hz, 2.1–2.0 (H-4e)[c]	3.10–2.95 (H-5a)[d]	7.2–7.1 (m)	3.45 (s)
						2.9–2.7 (H-5e)[f]		
		TB	4.40 and 5.19 (AB pattern), ^2J = −15.9 Hz	4.83 (dd), ^3J = 9.5 and 5.0 Hz[e]	2.2–2.0[e]	3.1–2.7[d,f]	7.2–7.1 (m)	3.45 (s)

[a] "a" and "e" refer respectively to axial and equatorial protons. [b] The multiplicity of this signal cannot be seen because of overlap with the methoxy signal. [c] The 4e protons of the Ca and Ce forms and the two 4 protons of the TB form are superposed. [d] H-5a of C_e and one H-5 of the TB form are superposed. [e] These coupling constants are not clearly resolved in Figure 3 but were measured on the resolution enhanced spectrum. [f] H-5e of Ce and one H-5 of the TB form are superposed.

Table III. Kinetic and Thermodynamic Parameters for Compounds 6 and 7

compd	solvent	confrmtn	popltn	$-\Delta G^{\circ}$ [b] (kcal/mol)	$\Delta G^{\ddagger}$ [b] (kcal/mol)
6	CH_3OCH_3	C	>98%	1.2 (C/TB, −120)	
(H, H)	CHF_2Cl	C	>98%	1.2 (C/TB, −120)	9.4 (C → C, −62)
7	CH_3OCH_3	Ca	61%[a]	0.43 (Ca/Ce, −120)	
(H, OCH_3)		Ce	15%	0.28 (Ca/TB, −120)	
		TB	24%	0.14 (TB/Ce, −120)	
	CHF_2Cl	Ca	50%[a]	0.23 (Ca/Ce, −120)	8.8 (TB → Ce, −90)
		Ce	23%	0.18 (Ca/TB, −120)	8.8 (TB → C_e, −130)
		TB	27%	0.05 (TB/Ce, −120)	11.1 (Ca → TB, −90)
					11.5 (Ca → TB, −130)

[a] Integration of C-1 and C-3 in the ^{13}C NMR spectra. [b] Temperatures are in °C.

contour plot. The horizontal line joining peaks 6–9 identifies protons coupled to 6 so that signal 7 at 1.9 ppm corresponds to C_eH-4e, signal 8 at 2.9 ppm to C_eH-5a, and signal 9 at 4.49 ppm to C_eH-3.

The correlation existing between 8 and 10 indicates that signal 10 at 2.65 ppm is associated with C_eH-5e. The signals of the two remaining methylene protons C_eH-1 will be identified later after those of the TB form **12** are assigned.

Integration of the complex signal centered at 2 ppm suggests that it includes the signals of the two TB H-4 protons. Furthermore, the left side of the signal clearly belongs to one of the TB H-4 protons as the above analysis has shown that it is not associated with protons of the C_a or C_e forms. The correlation between the corresponding diagonal peak 11 and the off-diagonal peak 12 leads to the assignment of 12 to TB H-3 at 4.65 ppm. Integration of the signals at 2.7 and 2.9 ppm suggests that the two TB H-5 signals overlap with those of C_e, namely C_eH-5a and C_eH-5e, as shown in Figure 4.

The intensity of the doublet at 4.3 ppm identifies it as TB H-1 and the correlation diagram involving 15 and 16 shows that the signal at ~5.0 ppm belongs to the other methylene proton TB H-1.

Finally, the remaining singlet at 4.52 ppm must belong to the two C_eH-1 protons as is supported by the results of integration. The results of the complete analysis of the 2D-COSY spectrum of **7** are given in Table II and illustrated in both Figures 3 and 4.

Returning now to the ^{13}C spectrum of **7** at −120 °C, our objective is to assign the various signals to the respective carbons in each of the three conformations. Heteronuclear selective decoupling techniques[6] at −120 °C were used together with two solvents, CHF_2Cl and CH_3OCH_3. The solvent change modifies the line intensities (conformer populations) without appreciably affecting their chemical shifts. In this way it was possible to identify all of the C-1–C-5 signals and especially those of C-4 and C-5 which lie close to each other. The aromatic carbon signals were assigned by comparison with those of **6** by using two solvents. The tentative assignment is summarized in Table I and illustrated partly in Figure 2.

The spectral modifications observed in Figure 2 identify interesting dynamic features for **7**. For example, the C-1 singlet at −20 °C broadens and splits into a doublet below −40 °C. At lower temperature the upfield component sharpens to give the C_a line whereas the downfield component broadens again to split below −80 °C into two lines identified as C_e and TB. This spectral change was simulated by computer calculations as will be discussed later.

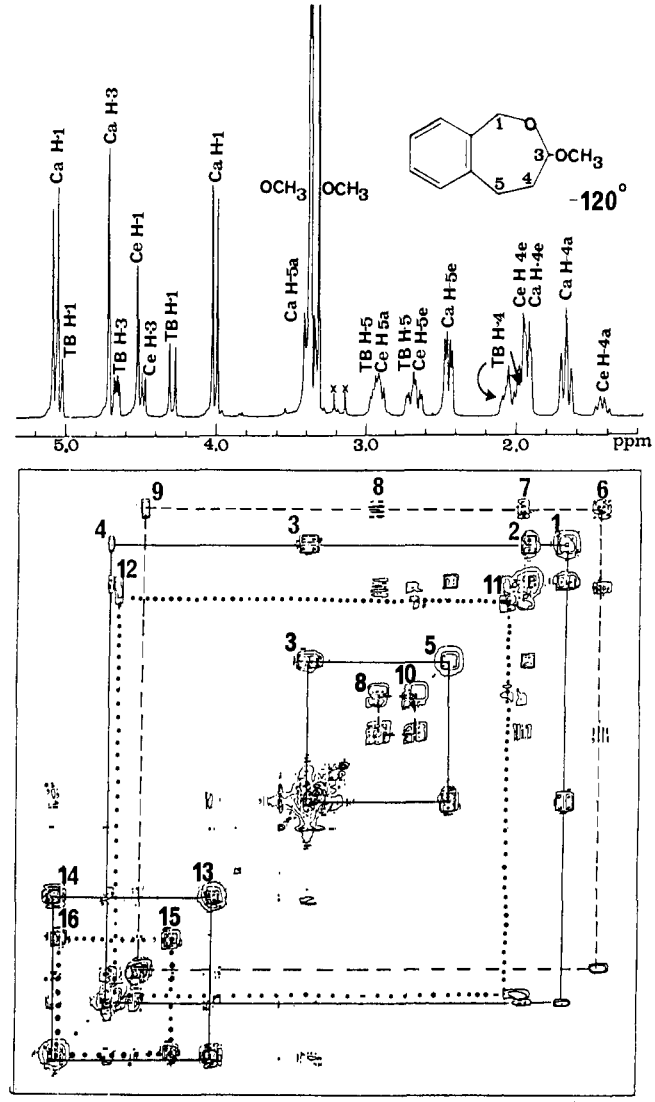

Figure 4. Partial 400.13-MHz ^1H NMR 2D COSY spectrum of **7** at −120 °C in CF_2Cl_2 (× denote impurities). Discontinued (– – –), continued (—), and dotted lines (···) correspond respectively to conformers C_e, C_a, and TB.

Discussion

Conformations of the Seven-Membered Rings. The analysis of the ^1H NMR spectrum of **6** at −120 °C (Figure 1 and Table II) shows clearly that its stable conformation is the chair **9**. Confirmation is also provided by the ^{13}C chemical shifts of C-1. Reference parameters for C and TB are provided by the benzodioxepin **1** which shows signals for the two forms at −120 °C in CHF_2Cl. Thus, it was reported[1] that the characteristic C-1 chemical shift is 76.25 ppm for C while for TB it is 70.38 ppm. The C-1 chemical shift of **6** is found to be 75.70 ppm at −130 °C in CHF_2Cl, in agreement with expectation for the chair conformation. Further characterization of the chair form is provided by the vicinal coupling constants determined for **6** at −125 °C. Large values of 13.0 and 12.5 Hz are determined for $^3J_{4a,5a}$ and $^3J_{4a,3a}$ respectively while $^3J_{4e,5e}$ is found to be 5.4 Hz. The other vicinal couplings are not resolved and are probably less than 2 Hz. These values are very similar to those found for benzocycloheptene[9] for which $^3J_{4a,5a}$ = 12.6 and $^3J_{4e,5e}$ = 6.6 Hz while $^3J_{4a,5e}$ and $^3J_{4e,5a}$ are both 1.1 Hz. The larger values for $^3J_{4e,5e}$ indicate ring puckering.[9]

In contrast, the spectral analyses of the ^1H and ^{13}C NMR spectra of **7** shows that it exists as a mixture of three conformers

(9) St-Jacques, M.; Vaziri, C. *Org. Magn. Reson.* **1972**, 4, 77.

C_a (**10**), C_e (**11**), and TB (**12**) whose proportions are summarized in Table III. In addition, ^1H coupling values of **7** reported in Table II show that, for C_a, $^3J_{4a,5a} = 14.0$ and $^3J_{4e,5e} = 5.5$ Hz while for C_e, $^3J_{4a,5a} = 12.0$ Hz. No vicinal coupling is resolved for TB. It is therefore not possible to use coupling constants to determine which of the two TB structures, **12a** or **12b**, is favored.

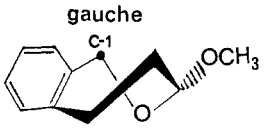

12a

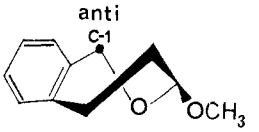

12b

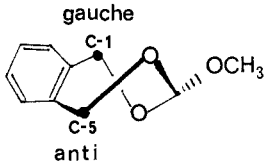

13

It is known that **4** exists in the TB form depicted by **13**. The reported[1] chemical shifts for the benzylic carbons vary according to their relationship to the methoxy substituent, and the signal of C-1 (gauche to OCH_3) appears at 62.57 ppm in CHF_2Cl at −150 °C while that of C-5 (anti to OCH_3) is located at 67.84 ppm. The fact that the analogous benzylic chemical shift of **7** is 63.15 ppm in CHF_2Cl at −120 °C indicates that the methoxy group in **7** is gauche to C-1 in agreement with **12a** being the predominant TB form.

The chemical shifts of the benzylic protons of **7** are also characteristic of each conformation. Table II and Figure 4 show that for the C_e form **11** both H-1a and H-1e have similar chemical shifts giving rise to the singlet observed at 4.52 ppm. On the other hand, the C_a form **10** gives an AX pattern with signals separated by 1.06 ppm. By comparison, the two H-1 protons of TB are separated by 0.75 ppm, suggesting that the relationship between OCH_3 and the methylene protons H-1 of TB is similar to that in C_a where OCH_3 is gauche to the benzylic C-1 carbon. Thus both ^1H and ^{13}C parameters point to **12a** as the predominant form of TB.

Finally, the so-called α, β, and γ parameters defined for substituents in acylic and cyclic systems[6,10] are useful to compare the C_a and C_e forms of **7** with those of the six-membered analogue **8**. Table I shows that the differences for the α effects in CHF_2Cl are 9.1 for **7** and 5.7 ppm for **8**. The source of the divergence lies mainly with the smaller α values for the C_a form of **7**.

Because the γ parameter has received most attention from a stereochemical point of view, the differences noted between **7** and **8** undoubledly reflect largely on the different degree of ring puckering for each ring as this feature changes the dihedral angular relationship between the substituent and the γ carbons C-1 and C-5. Such a relationship has been analyzed earlier by Lambert[11] for six-membered rings and St-Amour[2] for seven-membered cyclic compounds. Thus the larger γ-gauche values for the C_a form of **7** are in line with expectation for the reduction in the dihedral angles of the seven-membered ring. Similarly, the larger γ-anti values for the C_e form of **7** relative to **8** could result in large part from a reduced dihedral angle.

Conformational Averaging Processes. The spectral change in Figure 1 yields an activation energy ($\Delta G^{\ddagger}$) of 9.4 kcal/mol for **6** for the chair inversion by using a transmission coefficient of $^1/_2$ in the Eyring equation.[12] This value is significantly smaller than that determined for the same process in benzocycloheptene[9] (10.7 kcal/mol) and comparable to that of 3-oxabenzocycloheptene[13] (9.5 kcal/mol).

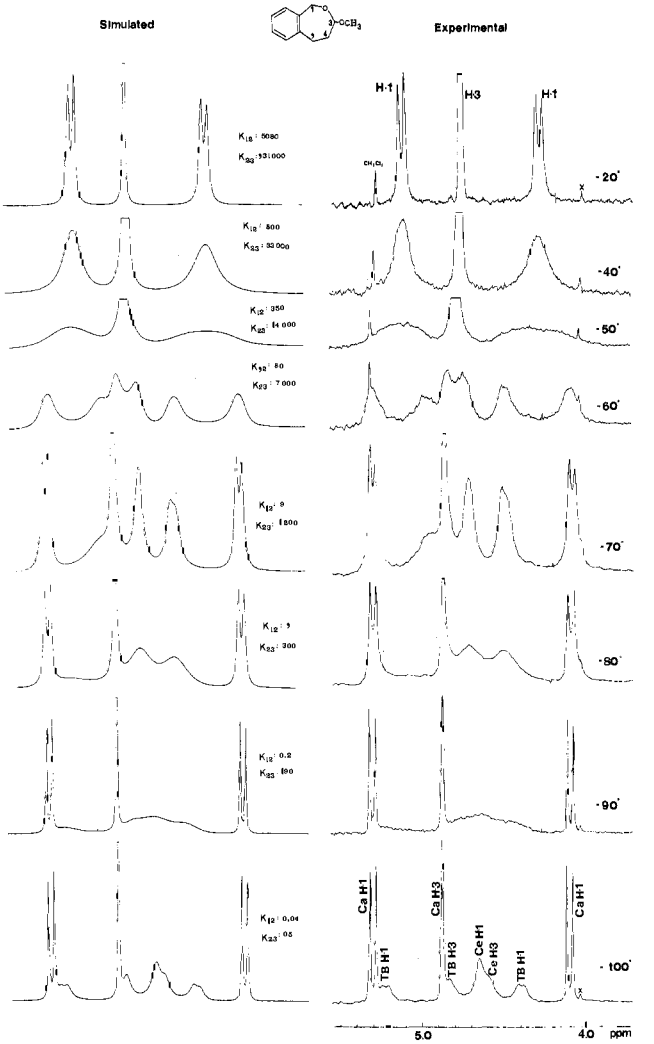

Figure 5. Partial ^1H NMR spectra of the H-1 and H-3 signal change at low temperature for compound **7**. Experimental (right) and matching calculated spectra (left).

Scheme I

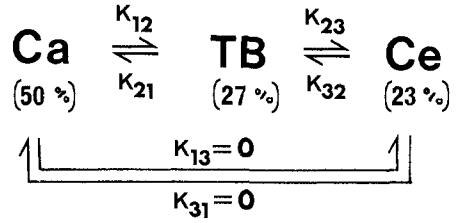

Because of the presence of three conformations in significant amounts for **7** and the observation of two spectral changes, its kinetic parameters cannot be obtained directly from approximate equations and require a complete line shape analysis. The variable temperature ^1H NMR spectra of **7** were therefore calculated with a slightly modified version of the DNMR-2 computer program.[14]

Scheme I illustrates the exchange modes involving the three different conformations of **7** in a ratio of 50:27:23 in CHF_2Cl.

(10) Subbotin, O. A.; Sergeyev, N. M. *J. Am. Chem. Soc.* **1975**, *97*, 1080.
(11) Lambert, J. B.; Vagenas, A. R. *Org. Magn. Reson.* **1981**, *17*, 265.
(12) (a) Kost, D.; Carlson, E. H.; Raban, M. *J. Chem. Soc., Chem. Commun.* **1971**, 656. (b) Eyring, H. *Chem. Rev.* **1935**, *17*, 65.
(13) Canuel, L.; St-Jacques, M. *Can. J. Chem.* **1974**, 52, 3581.
(14) (a) Binsch, G. *J. Am. Chem. Soc.* **1969**, *91*, 1304. (b) Ménard, D.; St-Jacques, M. *J. Am. Chem. Soc.* **1984**, *106*, 2055.

Scheme II

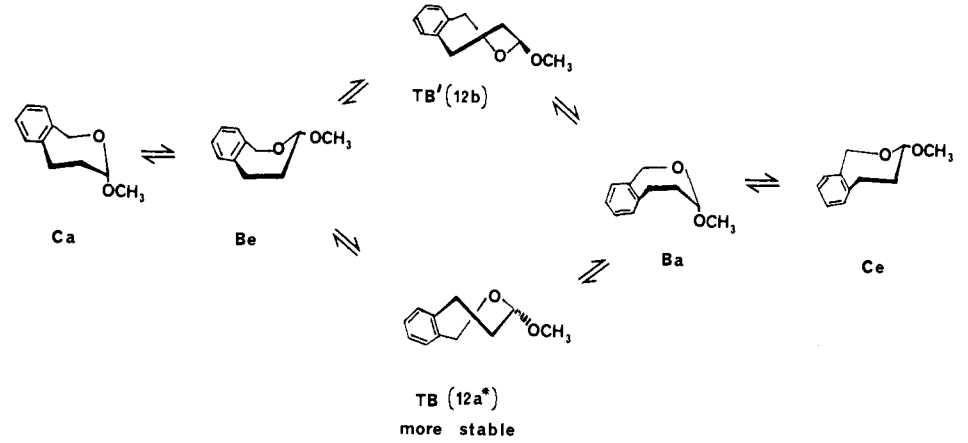

For each one, three protons are considered: the two methylene H-1 and H-3. ^2J coupling between the H-1 protons is considered explicitly whereas coupling constants with H-4 and H-5 are accounted for by line-broadening because the low-temperature spectrum of **7** at −120 °C (Figure 3) shows no splitting attributable to them. Furthermore, the calculations assume that, if **12b** were present, the interconversion of the two possible TB forms, **12a** and **12b**, is rapid and that the transformation of C_a into C_e necessarily proceeds via the boat and twist-boat family of conformations, i.e., $k_{13} = k_{31} = 0$ in Scheme I. The spectrum at −100 °C in Figure 5 shows the chemical shifts of the nine protons involved. Both C_eH-1 protons are assigned identical chemical shifts because they give a singlet at −120 °C. Finally, the conformation populations and NMR parameters were kept constant for all temperatures at which spectra were calculated.

Various trial calculations have shown that the itinerary of the H-1 protons is as follows: C_a H-1 (5.28 ppm) to TB H-1 (5.19 ppm) to C_e H-1 (4.65 ppm) and C_a H-1 (4.11 ppm) to TB H-1 (4.40 ppm) to C_e H-1 (4.65 ppm). Best values for the rate constants at each temperature in Figure 5 were obtained by trial and error method by using visual comparison of calculated and experimental spectra as test.

Plots of ln (k/T) vs. $1/T$ for k_{12} and k_{23} which represent, respectively, $k_{C_a \rightarrow TB}$ and $k_{TB \rightarrow C_e}$ yield $\Delta G^{\ddagger}$ values of 11.1 and 8.8 kcal/mol at −90 °C and 11.5 and 8.8 kcal/mol at −130 °C by using a transmission coefficient of 1. These values are summarized in Table III. In addition, $\Delta H^{\ddagger}$ and $\Delta S^{\ddagger}$ parameters were determined from the data by using standard methods.[15] Thus for $C_a \rightarrow$ TB, $\Delta H^{\ddagger} = 13.2$ kcal/mol and $\Delta S^{\ddagger} = 11$ eu while for TB $\rightarrow C_e$, $\Delta H^{\ddagger} = 8.7$ kcal/mol and $\Delta S^{\ddagger} = -0.05$ eu. Confirmation of the validity of k_{12} and k_{23} determined above is provided by the successful calculation of the C-1 spectral change of **7**, shown in Figure 2, with the same parameters.

Hence at −80 °C, the $C_a \rightleftharpoons$ TB process is slow on the NMR time scale while TB $\rightleftharpoons C_e$ still proceeds at an intermediate rate. As a consequence the C_a spectral lines of **7** are narrow while those of the TB and C_e forms are broad.

Scheme II shows the detailed interconversion pathways and suggested mechanism. We assume as was the case for benzocycloheptene,[16] that the transformation from the C forms to TB involves a C-3 flipping motion, so that C_a becomes B_e which can twist into either TB′ **12b** or TB **12a*** where the symbol * indicates a mirror image to structure **12a** presented in a previous section and shown to be the more stable of the two TB forms.

The kinetic parameters therefore indicate that the enthalpy of activation of the $C_a \rightarrow$ TB conversion is about 4.5 kcal/mol higher than that of the TB $\rightarrow C_e$ process. The interpretation of these parameters is not straightforward as they may refer largely to transition-state properties.

The Anomeric Effect in 7. Consequences of the anomeric effect have been the subject of numerous studies in six-membered rings.[17] First discovered from a study of pyranose sugars,[18] the concept has been extended to tetrahydropyran derivatives[4,19] such as **8** in which it refers to the axial preference of the electronegative substituent.

Several theories have been proposed to explain the origin of this phenomenon. The conformational features of molecules exhibiting the generalized anomeric effect (those containing the C–Y–C–X fragment where X and Y are heteroatoms) are now thought to be governed largely by a combination of two factors: (1) a stereoelectronic interaction between the lone pair of Y (oxygen for **7** and **8**) and the antibonding orbital of the adjacent C–X bond (namely n–σ^*)[5,20] and (2) electrostatic or dipole–dipole interactions.[21] Unfortunatly, the relative importance of each contribution is difficult to assess quantitatively and is still a matter of discussion and investigation.

In **8**, for example, two types of stereoelectronic interactions are important: the first one involves a lone pair from the ring oxygen as donor while the second one involves a lone pair from the methoxy group as donor. This later interaction is at the origin of the so-called exo anomeric effect.[5,22] The convergence of stereoelectronic and electrostatic interactions have been shown[5,23] to account for the accrued axial preference for **8** whose two stable conformations are **14** (C_a) and **15** (C_e).

In contrast, few example of seven-membered cyclic molecules exhibiting the anomeric effect have been studied. Data and arguments discussed in the preceeding sections show that **7** exists as a mixture of three conformations: C_a, C_e, and TB **12a**. Of these, the geometries of C_a and TB **12a** allow effective stabilizing n $\rightarrow \sigma^*$ interactions involving a ring oxygen lone pair antiperiplanar to the exo C–O bond. By comparison, no such interaction is possible in the C_e form. Furthermore, n–σ^* interactions involving a lone pair from the methoxy oxygen (associated with the exo anomeric effect) determine the preferred arrangement about the exo C–O bond of **7** (as for **8**). Thus structures **16**, **17**, and **18**, each containing the ring O–C bond gauche to the O–CH_3

(15) (a) Sandström, J. *Dynamic NMR Spectroscopy*; Academic Press: New York, 1982. (b) Jackman, L. M.; Cotton, F. A. *Dynamic Nuclear Magnetic Resonance Spectroscopy*; Academic Press: New York, 1975.

(16) (a) Favini, G.; Nava, A. *Gazz. Chim. Ital.* **1974**, *104*, 621. (b) Favini, G.; Nava, A. *Theor. Chim. Acta* **1973**, *31*, 261. (c) Allinger, N. L.; Sprague, J. T. *J. Am. Chem. Soc.* **1971**, *94*, 5734.

(17) *Anomeric Effect, Origin and Consequences*; Szarek, W. A., Horton, D., Eds.; ACS Symp. Ser. **1979**, *87*.

(18) (a) Edward, J. T. *Chem. Ind.* **1955**, 1102. (b) Lemieux, R. V. *Pure Appl. Chem.* **1971**, *25*, 527 and references cited therein.

(19) Franck, R. W. *Tetrahedron* **1983**, *39*, 3251.

(20) (a) Box, V. G. S. *Heterocycles* **1984**, *22*, 891; **1982**, *19*, 1939. (b) Wolfe, S.; Whangbo, M. H.; Mitchell, D. J. *Carbohydr. Res.* **1979**, *69*, 1.

(21) (a) Tvaroska, I.; Bleha, T. *Can. J. Chem.* **1979**, *57*, 424. (b) Vishveshwara, S.; Rao, V. S. R. *Carbohydr. Res.* **1982**, *104*, 21.

(22) (a) Lemieux, R. U.; Pavia, A. A.; Martin, J. C.; Watanabe, K. A. *Can. J. Chem.* **1969**, *47*, 4427. (b) Pĕrez, S.; Marchessault, R. H. *Carbohydr. Res.* **1978**, *65*, 114.

(23) (a) Kaloustian, M. K. *J. Chem. Ed.* **1974**, *51*, 777, and references cited therein. (b) Tvaraska, I.; Bleha, T. *Collect. Czech. Chem. Commun.* **1980**, *45*, 1883.

14 15

16 17 18

bond, allow for maximum n–σ^* stabilization while minimizing steric repulsions.

The above analysis therefore reveals that ring conformations of both C_a **16** and TB **18** are stabilized by anomeric and exo anomeric n–σ^* interactions while for C_e **17** only the exo interaction is possible.

With regards to the dipole–dipole contribution to conformational energy, we can consider qualitatively the interaction of the two dipoles bisecting[24] the C–O–C angles in each of **16**, **17**, and **18**. It is seen that the dipoles are antiparallel in both C_a **16** and TB **18** which are then stabilized by this interaction.[23,25] In C_e **17**, on the other hand, the dipole moments are oriented in the same direction and are destabilizing. Thus, the effects of both stereoelectronic and dipolar interactions involving the substituent converge and account for the accrued stability of the TB form of **7** relative to the parent compound **6** for which no TB conformation is detected. A more complete account of dipolar interactions should take into consideration the dipole moment of the benzo group[26] as will be done below.

In six-membered tetrahydropyrans, the term "anomeric effect" refers to the observed stability of axial electronegative 2-substituents relative to the expected stability predicted on steric grounds[19] for the equatorial location. Attempts to quantify the anomeric effect experimentally have presented much uncertainty. Deslongchamps and co-workers estimated a minimum value of 1.4 kcal/mol from spiro compounds[27] while Franks[19] argues in favor of a value of 2.1 kcal/mol which compares favorably with a calculated value of 2.8 kcal/mol.[20b] It now seems clear that a generally valid experimental value for the anomeric effect is not to be expected[28] as it will depend on ring geometry and competing steric interactions. The situation for **7** is even more complex because of the presence of three conformations. Nevertheless it is instructive to compare **7** and **8** where possible.

The C_e:C_a ratios, calculated for **7** by using data reported in Table III and from existing data[4b] for **8**, are 0.66 for **8** and 0.54 for **7** in CHF_2Cl whereas in CH_3OCH_3 the values become 0.19 and 0.39. A similar trend therefore exists for both compounds: C_a predominates in each solvent and more so in the less polar dimethyl ether solvent.

It will be recalled that a solvent change associated with increased polarity (such as CH_3OCH_3 to CHF_2Cl) modifies conformational distributions through the attenuation of intramolecular electrostatic interactions (E_D) and the preferential solvation (E_S) of the more polar conformation.[23] Because the C_e form is more polar, it is better solvated by CHF_2Cl, and because electrostatic repulsion of the dipoles is stronger in C_e, its attenuation in CHF_2Cl also favors C_e.

In addition, it has been suggested that solvation of the lone pair of oxygen might weaken the n–σ^* interaction.[29] This perturbation would also favor C_e relative to C_a. The relative magnitude of the solvation change on dipolar interactions and orbital interactions, the two contributions to the anomeric effect, has not yet been resolved.[23b] Our hypothesis is that perturbation of electrostatic interactions is more important. A change in this component can therefore compensate or overbalance the orbital interaction which is always stabilizing.

Hence, the changes in the C_e:C_a ratios for **7** and **8** given above are compatible with predictions from considerations of E_D and E_S. However, the smaller solvent perturbation noted for **7** relative to **8** may result from the presence of the additional dipole associated with the aromatic ring. Indeed it has been found[26] that 5-methoxybenzocycloheptene responds to a solvent change in a manner similar to **7**. Thus, the net result of the three dipoles appears to make the C_e form of **7** less polar and its dipolar destabilization smaller. As a consequence the solvent perturbation is attenuated in **7** since both E_D and E_S are less important than for **8**.

The solvent change from CH_3OCH_3 to CHF_2Cl causes very little change in the TB amount possibly indicating that it possesses a very small net dipole moment and that the E_S term is small.

It should be recalled that two forms are possible for TB, and the more stable one **12a** is expected to be less polar than **12b**. The solvent effect on ^{13}C chemical shifts (Table I) does not indicate a shift from **12a** to **12b** in agreement with a small overall polarity for the TB form. Analysis of a molecular model of **12a** suggests that the dipole orientations are such that the net E_D interaction should be small. Therefore, the fact that the TB amount is slightly increased on changing solvent (CH_3OCH_3 to CHF_2Cl) supports our hypothesis that the intracyclic n $\rightarrow$ σ^* interaction is not appreciably perturbed by the solvent change.

The extent of TB stabilization brought about by methoxy substitution in **6** cannot be determined from our data since no NMR signals are detected for this form in the parent compound. Calculations for cycloheptene suggest that the energy difference between C and TB is in the range 0.6–1.7 kcal/mol,[16] while for benzocycloheptene they suggest that TB is more stable than C by 3–4 kcal/mol.[16a] Consequently, the fact that methoxy substitution makes the TB energy comparable to that of the C_a and C_e forms suggests that appreciable stabilization is associated to the anomeric effect in the seven-membered TB ring. Indeed, the great flexibility of the TB form probably allows it to adopt a geometry with the ring oxygen lone pair antiperiplanar to the exo C–O bond allowing for maximum stabilization. By comparison, the puckering of the seven-membered C_a form discussed earlier causes some departure from antiperiplanarity so that overlap is less effective and stabilization resulting from the n–σ^* interaction is reduced.

Our results therefore provide a valuable illustration of consequences of the anomeric effect not manifested in six-membered rings. The stabilization by a single substituent of a ring conformation different from that observed for the parent compound could also occur in larger flexible rings for which the data obtained for **7** may have some predictive value.

Experimental Section

The variable temperature ^1H NMR spectra were recorded at 400.13 MHz on a Bruker WH-400 spectrometer, located at the "Laboratoire Régional de RMN à haut champ" in Montreal. Temperatures were determined directly by using the B-VT-100 unit. Verification using a calibrated copper-constantan thermocouple inside a solvent-containing NMR tube indicates that the low temperatures reported are known within ±3°. The samples were studied as solutions in chlorodifluoromethane (15–20 mg in 0.55 mL of solution) containing 18% of CD_2Cl_2 (for locking purpose) and a small quantity of Me_4Si in 5-mm tubes which had been degassed and sealed. The following instrumental parameters are typical: flip angle = 10°; SW =5000 Hz; data size = 16 K data points and zero filled to 32 K; acquisition time = 1.64 s. Gaussian multiplication was applied. The number of scans varied from 200 to 500.

The variable temperature ^{13}C NMR spectra were recorded at 100.62 MHz on the same Bruker WH-400. The samples were studied as solu-

(24) Jeffrey, G. A.; Pople, J. A.; Radom, L. *Carbohydr. Res.* **1972**, *117*, 25.
(25) Jeffrey, G. A.; Pople, J. A.; Brinkley, J. S.; Vishveshwara, S. *J. Am. Chem. Soc.* **1978**, *100*, 373.
(26) Mĕnard, D.; St-Jacques, M. *Tetrahedron* **1983**, *39*, 1041.
(27) Deslongchamps, P.; Rowan, D. D.; Pothier, N.; Saunders, J. K. *Can. J. Chem.* **1981**, *59*, 1105.
(28) Fuchs, B.; Schleifer, L.; Tastakovsky, T. *Nouv. J. Chim.* **1984**, *8*, 275.
(29) David, S.; Eisenstein, O.; Hehre, W. J.; Salem, L.; Hoffmann, R. *J. Am. Chem. Soc.* **1973**, *95*, 3806.

tions in chlorodifluoromethane and in dimethyl ether (130–150 mg in 2.2. mL of solution) containing 18% of CD_2Cl_2 (for locking purpose) and a small quantity of Me_4Si in 10-mm tubes which had degassed and sealed. The following instrumental parameters are typical: flip angle = 60–90°; SW = 20 000 Hz; data size = 16 K or data points and acquisition time = 0.41 s; number of scans = 500–2000; power decoupler (attenuation 5 dB on high range of the standard decoupler). The NMR data were treated by an exponential multiplication with LB varying from 1 to 6. A delay of 0.1–0.2 s was added between pulses for the spectra used for integration.

The rate constants were determined at the coalescence temperature by using the equation $k = \pi\Delta\nu/\sqrt{2}$ for singlet to doublet splitting in ^{13}C NMR spectra; this equation is known to give acceptable approximation even in the case of lines of unequal intensities.[12,15] The equation $k = \pi(\Delta\nu^2 + 6J^2)^{1/2}/\sqrt{2}$ was used for singlet to AB ^1H NMR spectral change. The free-energy barriers ($\Delta G^{\ddagger}$) were calculated from standard equations by using a transmission coefficient of $^1/_2$ or 1 one (vide infra).

Determinations of activation parameters of **7** were done by calculation of spectra at low temperature by using a slightly modified version of the DNMR-2 program on a CDC Cyber 173 computer.[1] The simulations were done by a visual comparison of the calculated and experimental spectra. Free energies of activation were calculated from a $\ln k/T$ vs. $1/T$ plot by using the Eyring equation.[15] Calculations of $\Delta S^{\ddagger}$ and $\Delta H^{\ddagger}$ were carried out from rate data obtained at several temperatures. The complete treatment was carried out by using standard procedures.[15] The two-dimensional ^1H NMR COSY experiment[8] was carried out with the standard Bruker 2D software and equipment by using the following pulse sequence: RD-90°-t_1-90°-t_2 (F1D). A spectral width of 2500 Hz and quadrature detection were used to collect a 128 F1D × 2K data matrix by using 16 scans. Zero filling gave a 1K × 2K matrix affording a digital resolution of 2.44 Hz/Pt. A sine bell square function was applied in both dimensions and absolute display was used.

1,3,4,5-Tetrahydro-2-Benzoxepin (6). This compound was prepared by using the method described by Rieche and Gross.[30] The procedure was slightly modified as follows: the intermediate chloromethyl 3-phenylpropyl ether was not distilled but conserved by adding some $CaCl_2$ as drying agent. In our hands heating led to apparent dimerization. The product was flash chromatographed on silica gel[31] and characterized as follows: ^1H and ^{13}C NMR spectra (Figure 2, Table II); mass spectrum EI; calcd for $C_{10}H_{12}O$ 148.0888, found 148.0885.

3-Methoxy-1,3,4,5-Tetrahydro-2-Benzoxepin (7). Compound **7** was prepared as previously described.[7] Its ^1H NMR was found to be identical with that reported, and the ^{13}C NMR spectrum (Figure 2 and Table I) confirms its identity.

Acknowledgment. We acknowledge the assistance of Dr. M. T. Phan Viet, mananger of the "Laboratoire Régional de RMN á haut champ" in Montréal. We are thankful for financial assistance from the Natural Sciences and Engineering Research Council of Canada.

Registry No. 6, 5698-85-1; 7, 87751-23-3; 8, 6581-66-4.

(30) Rieche, A.; Gross, H. *Chem. Ber.* **1961**, *95*, 91.
(31) Still, W. C.; Kahn, M.; Nitra, A. *J. Org. Chem.* **1978**, *43*, 2923.

Surface Site Distributions by Solid-State Multinuclear NMR Spectroscopy. Pyridine Binding to γ-Alumina by ^{15}N and ^2H NMR

Paul D. Majors and Paul D. Ellis*

Contribution from the Department of Chemistry, University of South Carolina, Columbia, South Carolina 29208. *Received August 25, 1986*

Abstract: The surface preparation dependent interactions of pyridine with γ-alumina are explored with solid-state ^{15}N and ^2H NMR spectroscopies. The observation of pyridine-^{15}N adsorbed to the surface reveals two resonances which are both characteristic of pyridine participating in a Lewis acid–base complex. These resonances display only partial tensorial averaging, and full information about the motionally averaged tensors is derived from magic angle spinning sideband simulations. Both resonances are assigned to complexes containing coordinatively unsaturated surface aluminum cations which occupy tetrahedral and octahedral sites in the defect spinel lattice. The relative distributions of tetrahedral and octahedral Lewis acid sites are determined as a function of surface preparation conditions, and the results are used with a simple surface preparation model to calculate the relative contribution of the various low index lattice planes to the composition of the surface. ^2H NMR line-shape studies of pyridine-α,α'-d_2 on γ-alumina indicate a heterogeneous distribution of pyridine motional species, which reflect the physical and steric characteristics of the surface binding sites. Quadrupolar spin–echo line-shape simulations for various motional models indicate the significant contributions of pyridines undergoing continuous diffusion or twofold ring flips about their twofold symmetry axis.

In the past several years we have been interested in the application of modern multinuclear solid-state NMR methods to probe the interactions between a sorbate and alumina surfaces. Our initial work involved the application of ^{13}C NMR to the chemisorption of amines, e.g., *n*-butylamine[1] and pyridine[2] to γ-alumina. In response to our pyridine work Ripmeester[3] published an interesting paper describing his ^{15}N NMR experiments utilizing ^{15}N-enriched pyridine on γ-alumina. In that paper he reported that pyridine forms two distinguishable Lewis acid complexes with γ-alumina. This is clearly an important observation which demonstrates the importance of utilizing more than a single "nuclear spin-label" when studying systems as complicated as these.

The importance of this observation, in addition to the difference in methods of γ-alumina preparation, prompted us to confirm his observations. Indeed we do confirm his results. In addition, we have determined the individual elements of the shielding tensor for each of the sites. With these data we have postulated that the two ^{15}N resonances represent pyridine nitrogen atom coordination to tetrahedral and octahedral Al^{3+} sites on the surface of the γ-alumina. The surface preparation dependence of the relative contribution of these resonances to the ^{15}N NMR spectra was observed and used to analyze the surface acid site distribution and to discuss the possible structure of the surface. Finally, the

(1) Dawson, W. H.; Kaiser, S. W.; Ellis, P. D.; Inners, R. R. *J. Am. Chem. Soc.* **1981**, *103*, 6780.
(2) Dawson, W. H.; Kaiser, S. W.; Ellis, P. D.; Inners, R. R. *J. Phys. Chem.* **1982**, *86*, 867.
(3) Ripmeester, J. A. *J. Am. Chem. Soc.* **1983**, *105*, 2925–2927.

0002-7863/87/1509-1648$01.50/0